

Imaging Soft Matter with the Atomic Force Microscope: Cubosomes and Hexosomes

Chiara Neto, Giovanni Aloisi, and Piero Baglioni*

Department of Chemistry, University of Florence, via Gino Capponi 9, 50121 Florence, Italy

Kåre Larsson

Camurus Lipid Research Foundation, Ideon, Gamma 1, Sölvesgatan 41, S-223 70 Lund, Sweden

Received: November 30, 1998; In Final Form: March 9, 1999

The atomic force microscope has been used to obtain images of colloidal dispersions of liquid crystal phases of cubic and hexagonal structures in water. Particle dimensions are consistent with dynamic light scattering and cryo-TEM data. The images we present in this work demonstrate the potential application of atomic force microscopy in revealing the morphology and structure of very soft matter in situ. This implies being able to detect possible structural modifications of the liquid crystalline phase due to in situ addition of enzymes, salts, polymers, etc. This kind of observation is not possible with other conventional high-resolution techniques.

Introduction

The most distinctive characteristic of surfactants is the capacity of their water mixtures to exist as liquid crystal phases. Liquid crystals behave as fluids, even though they are more structured than ordinary liquids: a long-range periodicity in two and three dimensions is evident from the narrow width of the X-ray lines. The liquid crystals remain very soft phases, and their structure and morphology have been studied by techniques that investigate their reciprocal lattice (small angle X-ray scattering, SAXS; small angle neutron scattering, SANS; etc.). The structure of these dispersed particles can also be detected with direct techniques that require frozen solutions (cryo-TEM, cryo-transmission electron microscopy). However, in this last case the extension of possible artifacts introduced upon the freezing process is not known.

The atomic force microscope (AFM) can image molecules in aqueous or other fluid environments by scanning a microscopic tip over a surface on which the molecules are bound.

The present work concerns the application of atomic force microscopy (AFM) to the visualization of stable colloidal dispersions of liquid crystal phases of cubic and hexagonal structure. We have chosen these dispersions because they have been previously well characterized by SAXS and cryo-TEM.^{1,2} The dispersions are constituted of cubic (CPDP) and hexagonal (HPDP) particles of submicron dimensions and have been named cubosomes for the cubic phase and, by analogy, hexosomes for the hexagonal phase. In this report, *these soft particles are visualized in situ for the first time by a direct technique such as AFM*, and the results are compared with those obtained by the classical quasielastic light scattering technique (QELS).

Hexosomes and cubosomes are colloidal dispersions of an inverted type of hexagonal (usually denoted H_{II})³ and bicontinuous cubic phase (usually denoted Q_{II}), respectively. The bulk hexagonal phase consists of hexagonally closed-packed infinite water cylinders covered by a lipid monolayer,^{2,3} and it may be

regarded as possessing two-dimensional long-range order. A plane passing through this structure perpendicular to the direction of the cylinders would reveal circular or hexagonal-shaped cross-sections, and the centers of adjacent cylinders lie at the vertexes of equilateral triangles. Six adjacent triangles which have in common a vertex form a hexagonal pattern. The hexagonal phase may be visualized as resulting from the break-up of the lamellar phase (infinite bilayers stacked one over the other in a one-dimensional long-range order structure) into cylindrical elements in consequence of dilution of the surfactant. The diameter of the cylinders is similar to the thickness of the bilayer, and their length is indefinitely long.

The bicontinuous cubic phase is the intermediate phase which often occurs between almost every other liquid crystal phase.⁴ The structure of one type may be visualized in the following way. Imagine spheres along the three axes *x*, *y*, and *z*. We let them touch and then fuse at the contacts. If the spheres of this network can be deformed and strive to minimize the total surface area like a soap film, increasing the outer pressure will shrink the surface and when outer and inner space is equal we have the P-surface and the surface minimal area.

The structure consists of infinite bilayers periodically curved in three dimensions,^{5,6} and the curvature is at every point as positive as it is negative (a saddle point, see Figure 1). This structure is a member of the family of “periodical minimal surfaces”, which have been described exactly by mathematical formulas.^{7–11}

Colloidal dispersions of these two inverted amphiphilic phases can be prepared. The submicron particles that constitute the dispersion will be called dispersed cubic particles and dispersed hexagonal particles, or simply, cubosomes (CPDP) and hexosomes (HPDP).

CPDP's similarity with liposomes suggests their applicability for drug delivery,^{5,12} and their possible biological relevance^{5,6} was one of the reasons motivating our studies.

It has been demonstrated¹³ that protein molecules (such as lysozyme) can be entrapped within the water channel system of the cubic structure. It has been observed¹⁴ that the cubic phase can serve as a model of the inner mitochondrial membrane and

* Correspondence and requests for materials to: Prof. Piero Baglioni, Department of Chemistry, via Gino Capponi 9, 50121 Florence, Italy. Phone: +39 55 275-7567; fax: +39 55 240865; e-mail: Baglioni@mac.chim.unifi.it.

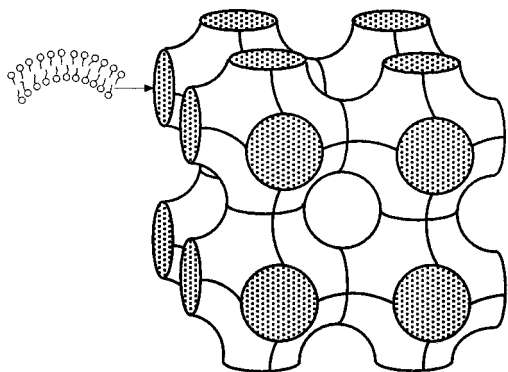


Figure 1. A view of a bicontinuous cubic phase structure. The arrangement of the bilayers within the bicontinuous structural surface is indicated.

that the packing parameter of monoolein decreases in a cubic phase and many other factors are modified upon protein (cytochrome-*c*) incorporation.

Razumas et al.¹⁵ constructed enzyme-based biosensors, where the enzyme is entrapped in a cubic liquid crystalline phase made of monoolein, and Landau et al.¹⁶ used lipidic cubic phases as transparent, rigid matrixes for investigating the structure and the functionality of membrane proteins. Portmann et al.¹⁷ found out that α -chymotrypsin, a water-soluble enzyme, retains its native conformation and exhibits enzymatic activity upon incorporation in the cubic phase.

The amphiphilic constituent of CPDP and HPDP, which are studied most, is glycerol monooleate (GMO). Landh found^{18,19} that an amphiphilic block copolymer is very efficient as a dispersing and stabilizing agent for inverted cubic phases. A nonionic triblock polymer, called Polaxamer 407, made of two side blocks of 98 units of poly(ethylene oxide) (PEO) and one central block of 67 units of poly(propylene oxide) (PPO) was used for this purpose.^{1,2,19} In mixtures of GMO and GTO (glycerol trioleate), a reversed hexagonal phase is formed.

The present work is mainly directed to the morphology of the stabilized particles. The particle morphology is characterized by combined dynamic light scattering (DLS) and AFM. The former technique provides indirect information on the particles' dimensions that are obtained through the analysis of the autocorrelation function, whereas with the latter, the morphology and size of the particles are directly observed.

Experimental Section

The glycerol monooleate (GMO) was a distilled monoglyceride (RYLO MG 90, Danisco Ingredients, Brabrand, Denmark) with the following fatty acid composition: oleic acid 92%, linoleic acid 6%, saturated acids 2%. The glycerol trioleate (GTO) was a high monosaturated sunflower oil (Trisun 80 SVO, Eastlake, Ohio). Polaxamer 407 was obtained from BASF (Germany).

The dispersion procedure has been described in a previous work.²

The cubic phase composition is 97 wt % of water and 3% of composition: amphiphilic part made of GMO (94%) and Polaxamer 407 (6%).

The hexagonal phase compositions are 97 wt % of water and 3% of composition: 94% GMO/GTO (88/12 wt ratio, respectively) and 6% Polaxamer 407, or 94% GMO/GTO (94/6 wt ratio, respectively) and 6% Polaxamer 407.

The samples of cubosomes and hexosomes were imaged with AFM as received without additional purification.

Being cubosome and hexosome polar particles on the surface, they can be readily adsorbed on a polar substrate such as muscovite mica. Freshly cleaved muscovite mica squares were used as substrate for the adsorption of the dispersions, and the samples were imaged under bidistilled water. Operating in water is not only necessary to study the liquid crystal phases in their original environment, it is also an efficient way to eliminate the undesirable and often destructive adhesion force that drives the tip toward the sample in consequence of adsorbed contaminant layers that cover the tips (i.e., water condensation) and samples when operating in air. Because both tip and cantilever are immersed in liquid, the applied force is more precisely known and controlled. Imaging forces in air are typically on the order of 10 times greater than imaging forces in liquid.^{20,21}

CPDP and HPDP were observed with a noncontact atomic force microscope and with a special scanner for liquid imaging. Silicon nitride microfabricated cantilevers with integrated pyramidal tips for noncontact imaging were supplied by Topometrix. Good particle images were not always easily obtained, and it was sometimes a challenge to obtain homogeneous particle distributions over the substrate. Images were taken with online filtering and subsequently processed by flattening to remove the background slope. Scan rates varied from 1 to 15 Hz per line. Information density of captured images was 200 pixels per line for 200 lines. The procedure for imaging the colloidal particles was the following: a few μL of the dispersion of cubosomes (3%) was placed on the freshly cleaved chip (2.5 cm \times 2.5 cm) of muscovite mica for 10 minutes. The mica surface was then abundantly rinsed with bidistilled water. Loosely bound material may indeed cause difficulties during imaging. The mica was then covered with 10–20 μL of bidistilled water. The sample was scanned in constant force mode with a Explorer TMX 2000 (Topometrix) using a 130 μm liquid scanner.

Results

CPDP and HPDP can be imaged in aqueous solution with a noncontact atomic force microscope. In noncontact mode, the AFM tip is oscillated at its resonant frequency: as the probe gets closer to the sample surface (a few nm or less from it), the interaction forces between the tip and the sample change both the oscillation amplitude and phase of the probe tip. These changes can be detected and used by a feedback loop to control the tracking of the probe over the surface. The distance between the scanning tip and the sample surface being so little, we cannot exclude some physical contact between the probe and the particle surface, possibly because of mechanic vibrations and environmental noise. The actual contact sometimes may cause limited damage to the particles (especially for the hexosomes); however, both in noncontact mode and in contact mode AFM certainly remains the less perturbative *in situ* imaging technique available. Moreover, with both cubosomes and hexosomes, slow scan rates and large scan sizes are generally more delicate to the soft particles.

Some of the presented images are given in a double version: the so-called internal sensor signal and the topographic signal. The former signal is gathered by detecting the sensor current (cantilever deflection) which can be converted into surface height information. The regions of the surface for which the signal is higher are highlighted in the AFM images with brighter colors. The latter signal represents voltage gradients used from the feedback system to control the piezos that guide the vertical position of the cantilever. Depending on the sample and on the scanning conditions, one of the two signals can provide more information than the other.

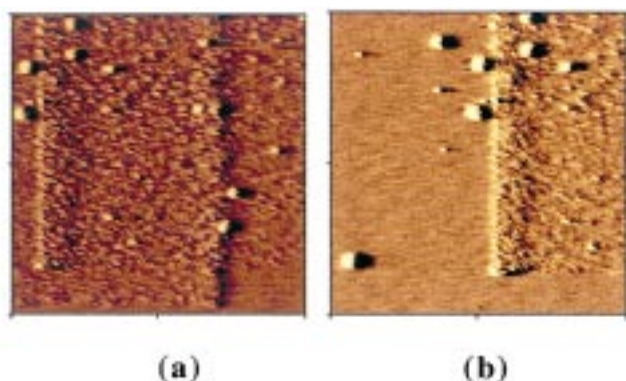


Figure 2. Noncontact AFM image of the dispersion of cubosomes on mica. (a) Image dimensions: $20.59\ \mu\text{m} \times 20.59\ \mu\text{m}$. (b) Image dimensions: $19.9\ \mu\text{m} \times 19.9\ \mu\text{m}$. The cubosomes in these images appear to have a side of dimensions varying between 300 and 750 nm and have a height on the substrate around 14–16 nm. The vertical lines visible in (a) and (b) are presumably cleavage planes of mica. Small objects visible in this and in the next figures are probably agglomerates of the degraded liquid crystal phase.

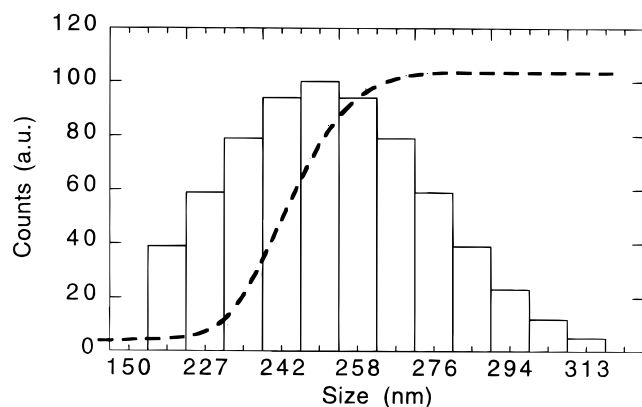


Figure 3. Size distribution of cubosomes obtained by the analysis of the autocorrelation function with the constrained regularization method (CONTIN). The autocorrelation function has been obtained by a Brookhaven 9000AT correlator and a Coherent Nd:YAG (532 nm) laser diode operating at 100 mW.

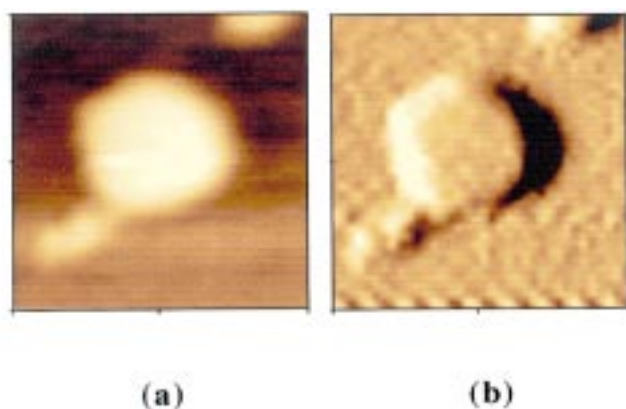


Figure 4. Noncontact AFM image of the dispersion of cubosomes on mica: (a) and (b) image dimensions $1.05\ \mu\text{m} \times 1.05\ \mu\text{m}$. (a) Topographic image. (b) Internal sensor image. The cubosome in these images appears to be of about $300 \times 300 \times 23\ \text{nm}$.

The many captured images of the cubosomes show a major portion of clearly faceted cubic particles, oriented with one side parallel to the mica surface, probably as a consequence of the drag experienced by the particles during the scanning of the tip. It was not possible to resolve the inner texture and periodicity that appear in cryo-TEM images and from X-ray

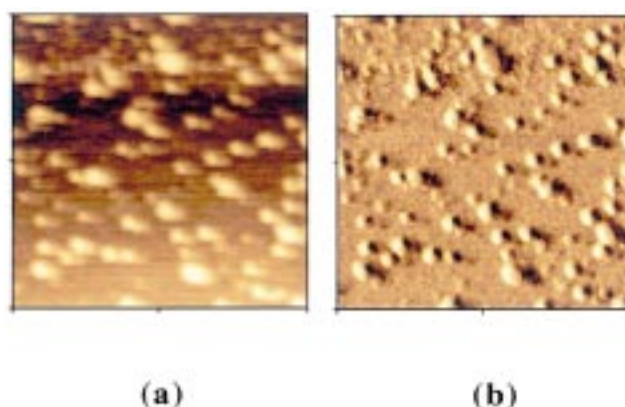


Figure 5. Noncontact AFM image of the dispersion of hexosomes (GMO/GTO:88/12) on mica: (a) and (b) image dimensions $4.01\ \mu\text{m} \times 4.01\ \mu\text{m}$. (a) Topographic image. (b) Internal sensor image. The hexosomes in these images appear to have mean dimensions of the sides around 150 nm and an height on the mica surface of 30–35 nm.

diffraction.^{1,19} The angles at the corners of the squares (in projection) sometimes do not appear clearly of 90 degrees. This appearance was also observed in previously published cryo-TEM images,¹ where vesicular structures were often found at the corners of the faceted particles, a consequence of the difficulty in terminating the structure at a point where three orthogonal planes meet.

The observed CPDP show a narrow size distribution with CPDP particles of about 300 nm. A similar size distribution appears from dynamic light scattering experiments made on the same samples (see Figure 3). The analyses of the results have been performed according to the nonnegative nonlinear least squares (NNLS)²² and the constrained regularization (CONTIN)²³ methods, which give similar size distributions for the cubosome solutions (mean particle diameter of 254 nm). We recall that the size distribution obtained by QELS is related to the equivalent hydrodynamic sphere described by the CPDP particle in fast tumbling.

The captured images of the HPDP show clearly faceted hexagonal particles. The number of the sides of the visualized hexagonal structures is not always equal to six as expected, a consequence of the orientation of the hexosome with respect to the mica surface and possibly of the friction exerted by the scanning of the tip (as mentioned before) on the sample. Moreover, the same portion of the sample could be scanned repeatedly without changing the image.

The hexagonal geometry is clearly distinguishable, especially from the nearly 120° inner angle. The main portion of the observed hexosomes was found having sides 200–300 nm long (mean lateral dimensions shorter than the cubosomes'), but a few of them also show 700 nm long sides.

The apparent height of the particles on the surface of the mica is between 13 and 40 nm, definitely below the expected height, which should be close to the lateral dimension. This is probably due to several factors. First, the oscillating tip might sink into the soft particles and the AC detection method of the noncontact AFM mode, which is sensitive to force gradients in a direction perpendicular to the sample surface, may underestimate their height over the mica surface. Moreover, the adsorption phenomenon of the particles on the mica surface may have a flattening effect.

Conclusions

For the first time, a direct investigation technique (atomic force microscopy) has been successfully applied to the inves-

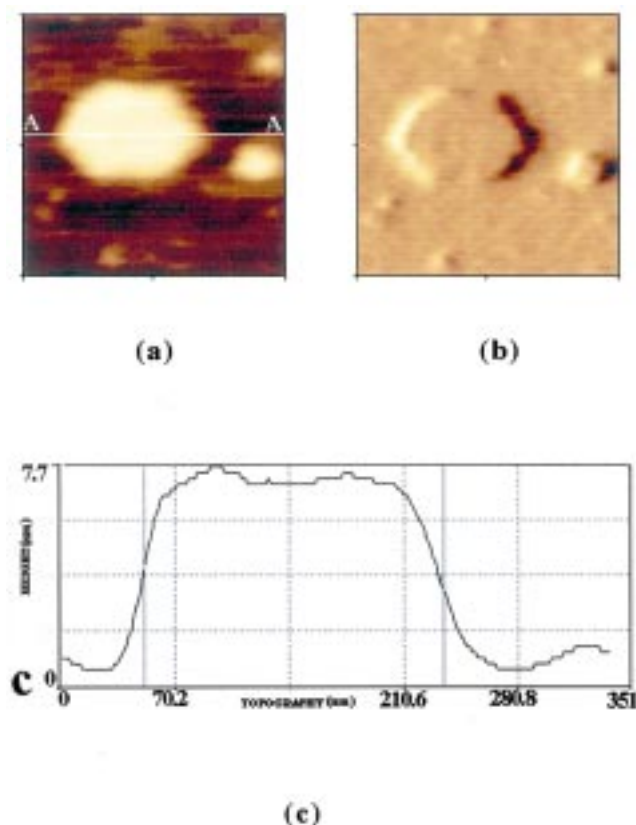


Figure 6. Noncontact AFM image of the dispersion of hexosomes (GMO/GTO: 94/6) on mica: (a) and (b) image dimensions $352.22 \text{ nm} \times 352.22 \mu\text{m}$. (a) Topographic image. (b) Internal sensor image. (c) Topographic plot of lateral dimensions vs vertical height (Z). The hexosome in these images appears to be 184 nm long along the AA segment and to have a height on the mica surface of 7.6 nm .

tigation in situ of the size and shape of submicron particles of very soft matter, cubosomes and hexosomes. Until now, in situ investigation of soft matter formed by nanometer particles was possible only by using scattering techniques that investigate the reciprocal lattice (small angle neutron or X-ray light scattering, etc.).

The importance of the in situ observation is in the possibility of directly observing liquid crystal structure modifications as a consequence of many factors, e.g., temperature variations or addition of enzymes, salts, proteins, polymers, etc. to the dispersion. A few examples of these previous studies have been cited before: it was found that α -chymotrypsin,¹⁷ a water-soluble enzyme, retains its native conformation and exhibits enzymatic activity upon incorporation in the cubic phase; enzyme-based biosensors¹⁵ can be constructed, where the

enzyme is entrapped in a cubic liquid crystalline phase made of monoolein; protein molecules (such as lysozyme) can be entrapped¹³ within the water channel system of the cubic structure; the cubic phase can serve as a model of the inner mitochondrial membrane,¹⁴ and protein (cytochrome-c) incorporation decreases the packing parameter of monoolein in a cubic phase and modifies many other factors; lipidic cubic phases may be used as transparent, rigid matrixes for investigating the structure and the functionality of membrane proteins;¹⁶ etc.

These are only a few of the many possible biological applications of the liquid crystalline phases, and it is clear that a noninvasive direct technique such as AFM will give a strong aid to future studies in this field.

Acknowledgment. Thanks are due to MURST, CNR, and Interuniversity Consortium for Large Interface Systems (CSGI) for financial support.

References and Notes

- (1) Gustafsson, J.; Ljusberg-Wahren, H.; Almgren, M.; Larsson, K. *Langmuir* **1996**, *12*, 4611–4613.
- (2) Gustafsson, J.; Ljusberg-Wahren, H.; Almgren, M.; Larsson, K. *Langmuir* **1997**, *13*, 6964–6971.
- (3) Seddon, J. M. *Biochim. Biophys. Acta* **1990**, *1031*, 1–69.
- (4) Fontell, K. *Colloid Polym. Sci.* **1990**, *268*, 264–285.
- (5) Larsson, K. *J. Phys. Chem.* **1989**, *93*, 7304–7314.
- (6) Lindblom, G.; Rilfors, L. *Biochim. Biophys. Acta* **1989**, *988*, 221–256.
- (7) Andersson, S.; Jacob, M. *Z. Kristallogr.* **1997**, *212*, 334–346.
- (8) Jacob, M.; Larsson, K.; Andersson, S. *Z. Kristallogr.* **1997**, *212*, 5–8.
- (9) Andersson, S.; Jacob, M.; Lidin, S.; Larsson, K. *Z. Kristallogr.* **1995**, *210*, 315–318.
- (10) Andersson, S.; Jacob, M.; Lidin, S. *Z. Kristallogr.* **1995**, *210*, 3–4.
- (11) Larsson, K.; Jacob, M.; Andersson, S. *Z. Kristallogr.* **1996**, *211*, 875–878.
- (12) Ljusberg-Wahren, H.; Nyberg, L.; Larsson, K. *Chem. Today*, June **1996**, 40–43.
- (13) Ericsson, B.; Larsson, K.; Fontell, K. *Biochim. Biophys. Acta* **1983**, *729*, 23–27.
- (14) Razumas, V.; Larsson, K.; Mieziš, Y.; Nylander, T. *J. Phys. Chem.* **1996**, *100*, 11766–11774.
- (15) Razumas, V.; Kanapienienė, J.; Nylander, T.; Engstrom, S.; Larsson, K. *Anal. Chim. Acta* **1994**, *289*, 155–162.
- (16) Landau, E. M.; Luisi, P. L. *J. Am. Chem. Soc.* **1993**, *115*, 2102–2106.
- (17) Portmann, M.; Landau, E. M.; Luisi, P. L. *J. Phys. Chem.* **1991**, *95*, 8437.
- (18) Landh, T. Thesis, University of Lund, 1992.
- (19) Landh, T. *J. Phys. Chem.* **1994**, *98*, 8453–8467.
- (20) Drake, B.; Prater, C. B.; Weisenborn, A. L.; Gould, S. A. C.; Albrecht, T. R.; Quate, C. F.; Cannell, D. S.; Hansma, H. G.; Hansma, P. K. *Science* **1989**, *243*, 1586–1589.
- (21) Cappella, B.; Baschieri, P.; Frediani, C.; Miccoli, P.; Ascoli, C. *Eng. Med. Biol.*, March–April **1997**, 58–65.
- (22) Lawson, C. L.; Hanson, R. J.; *Solving Least Square Problems*; Prentice Hall: Englewood Cliffs, NJ, **1974**.
- (23) Provencher, S. W. *Comput. Phys. Comm.* **1982**, *27*, 213–218.